Variable temperature neutron diffraction study of crystal structure and transport pathways in oxide ion conductors Bi12.5Ln1.5ReO24.5 (Ln=Lu, Er)

Hervoches, Charles; Greaves, Colin

DOI:
10.1016/j.ssi.2013.10.032

Document Version
Publisher's PDF, also known as Version of record

Citation for published version (Harvard):
Hervoches, CH & Greaves, C 2014, 'Variable temperature neutron diffraction study of crystal structure and transport pathways in oxide ion conductors Bi12.5Ln1.5ReO24.5 (Ln=Lu, Er)', Solid State Ionics, vol. 254, pp. 1-5. https://doi.org/10.1016/j.ssi.2013.10.032

Solid State Ionics 254 (2014) 1–5

Contents lists available at ScienceDirect

Solid State Ionics

journal homepage: www.elsevier.com/locate/ssi

Variable temperature neutron diffraction study of crystal structure and transport pathways in oxide ion conductors $Bi_{12.5}Ln_{1.5}ReO_{24.5}$ (Ln = Lu, Er)

Charles H. Hervoches *, Colin Greaves

School of Chemistry, The University of Birmingham, Edgbaston, Birmingham, B15 2TT, United Kingdom

ARTICLE INFO

Article history:
Received 25 March 2013
Received in revised form 12 September 2013
Accepted 17 October 2013
Available online 7 November 2013

Keywords:
Bismuth oxide
Fluorite structure
Oxide ion conductor
Neutron diffraction
Maximum entropy method
Diffusion path

ABSTRACT

Samples of highly conducting $Bi_{12.5}Lu_{1.5}ReO_{24.5}$ and $Bi_{12.5}Er_{1.5}ReO_{24.5}$ have been studied by neutron powder diffraction at room temperature for both phases and at 25 °C ≤ T ≤ 500 °C in the case of $Bi_{12.5}Er_{1.5}ReO_{24.5}$. Both materials crystallize in the cubic δ-Bi_2O_3 related system, space group Fm-3m. Changes in the oxygen sublattice at 25 °C ≤ T ≤ 500 °C have been investigated by the Rietveld and maximum entropy methods.

1. Introduction

The high ionic conductor δ-Bi_2O_3 crystallises in a defect fluorite related structure, space group Fm-3m [1]. Its crystal structure is typically described with cations occupying the *4a* (0 0 0) position and oxygens in *8c* (¼ ¼ ¼) with some interstitial oxygens shifted towards (½, ½, ½) [2], however slightly different systems to model the disordered distribution of the oxide ions have been proposed [3,4]. Its high ionic conduction is linked to the presence of ~25% oxygen ion vacancies in the structure [1,5]. The phase is stable only above 730 °C, and attempts to stabilise the high oxide ion conductor δ-phase at lower temperature have been the subject of numerous studies [6,7]. Amongst them, the stabilised δ-phase family of compounds with composition $Bi_{12.5}Ln_{1.5}ReO_{24.5}$ presents very high ionic conductivity at low temperature [8] and their detailed crystal structure characteristics appear to differ from those of Bi_2O_3 doped with rare-earth only. In these materials, rhenium is apparently tetrahedrally coordinated at the local scale [9], while in the related ordered phase both tetrahedral ReO_4^- and octahedral ReO_6^{5-} species are present [10,11]. To date NPD data have been obtained only for T ≤ 25 °C, and indicate significant differences in the O positions compared with conventional lanthanide stabilised phases: the interstitial oxygen position is significantly displaced and is thought to be related to the enhanced conductivity [8]. In the present study we investigate the crystal structure of the $Bi_{12.5}Ln_{1.5}ReO_{24.5}$ (Ln = Lu, Er) system and the change in oxygen sublattice for 25 °C ≤ T ≤ 500 °C in $Bi_{12.5}Er_{1.5}ReO_{24.5}$.

2. Experimental

Polycrystalline samples of $Bi_{12.5}Lu_{1.5}ReO_{24.5}$ and $Bi_{12.5}Er_{1.5}ReO_{24.5}$ have been prepared by traditional solid state synthesis from stoichiometric quantities of Bi_2O_3, Lu_2O_3/Er_2O_3, and NH_4ReO_4. The powders were thoroughly mixed and ground, and subsequently heated in air at 800 °C for 24 h with one intermediate grinding and allowed to cool slowly in the furnace.

X-ray powder diffraction (XRD) data were obtained at room temperature on a Siemens D5000 diffractometer operating in transmission mode (Ge primary beam monochromator giving Cu-Kα1 radiation, wavelength 1.5406 Å). Neutron powder diffraction (NPD) data of the samples were collected on the D2B diffractometer (wavelength 1.5943 Å) at the Institut Laue Langevin, Grenoble, France. Approximately 8 g of each material was loaded in a cylindrical vanadium can of 8 mm diameter for data collection at temperatures of 25 °C, 200 °C, 300 °C, 400 °C, and 500 °C.

Rietveld refinements were carried out using GSAS [12] with EXPGUI graphical user interface [13]. The nuclear density distribution was obtained by the maximum entropy method (MEM)/MEM-based pattern fitting (MPF) method using the program PRIMA [14] with 128 × 128 × 128 pixels in conjunction with Rietan-FP software [15].

* Corresponding author at: Department of Neutron Physics, Nuclear Physics Institute v.v.i., ASCR, CZ-25068 Řež, Czech Republic. Tel.: +420 266172034.
E-mail address: hervoches@ujf.cas.cz (C.H. Hervoches).

0167-2738/$ – see front matter © 2013 Elsevier B.V. All rights reserved.
http://dx.doi.org/10.1016/j.ssi.2013.10.032

Crystal structures and nuclear density distribution representations were drawn with VESTA [16].

For electrical measurements, dense sintered pellet of approximately 8 mm diameter and 2 mm thickness were prepared and silver electrodes painted on both surfaces. Conductivity was measured over the temperature range 200–600 °C by a.c. impedance spectroscopy with a Solartron SI 1260 impedance analyzer in the frequency range 1 Hz to 10^6 Hz.

3. Results and discussion

XRD data confirmed the phase purity of the samples. As with other lanthanide doped bismuth rhenium oxides, they both adopt the cubic *Fm-3m* space group, lattice parameter $a = 5.5592(1)$ Å and 5.5697(1) Å for $Bi_{12.5}Lu_{1.5}ReO_{24.5}$ and $Bi_{12.5}Er_{1.5}ReO_{24.5}$ respectively at 25 °C.

Conductivity measurement (Fig. 1) demonstrated the high conductivity of the materials with values close to the ones previously reported [8]. Both materials have conductivity higher than $Bi_{12.5}Y_{1.5}ReO_{24.5}$ but lower than $Bi_{12.5}Nd_{1.5}ReO_{24.5}$ and $Bi_{12.5}La_{1.5}ReO_{24.5}$. This follows the general trend of stabilized lanthanide doped δ-Bi_2O_3, which generally present higher conductivity with increased dopant ionic radius.

NPD data Rietveld refinements were performed using data from reference [8] based on δ-Bi_2O_3 crystal structure as a starting model. Lattice parameter variation with temperature deviates from linearity (Fig. 2), which might indicate of a redistribution of oxide ions.

In their study of pure and Y-doped δ-Bi_2O_3, Battle et al. [2] observed the presence of interstitial oxygens on *32f* (*xxx*) site in both cases, with another interstitial oxygen in *48i* (½ *x x*) and displacement of cations to the *24e* (*x 0 0*) *site* in the case of the Y-doped sample. Three oxygen positions (*8c*, *32f*, *48i*) were also reported with several lanthanide-doped Bi_2O_3 by Boyapati et al. [17] and Y-doped Bi_2O_3 by Abrahams et al. [18]; while in the $Bi_3Ta_{1-x}Nb_xO_7$ system some oxygens are located in *24d* (0.5, 0.25, 0.25) rather than the *48i* site [19].

Our Rietveld refinements of $Bi_{12.5}Ln_{1.5}ReO_{24.5}$ (Ln = Lu, Er) indicate that the cations occupy the *4a* (*0 0 0*) site and that anion positions can be modelled by partial occupancy of *8c and 32f* sites (Table 1) while possible occupancy of the *48i* position is less clear (Fig. 3).

Due to the complicated distribution of anions in these systems, we chose to represent it with nuclear densities obtained by the MEM/MPF methods instead of the classical split-atom system. The methods can provide precise nuclear/electron distribution, is less prone to termination ripples than Fourier methods, and can also give indications of conduction pathways [20].

After completion of the iterative MEM/MPF procedure, the reliability factors R_B (R-Bragg factor; also denoted by R_I) and R_F (R-structure factor) improved to final values of (%): $R_B = 4.091$, $R_F = 1.461$ ($Bi_{12.5}Lu_{1.5}ReO_{24.5}$, 25 °C); $R_B = 2.844$, $R_F = 1.024$ ($Bi_{12.5}Er_{1.5}ReO_{24.5}$, 25 °C); $R_B = 3.095$, $R_F = 1.342$ (200 °C); $R_B = 2.789$, $R_F = 1.373$ (300°); $R_B = 2.988$, $R_F = 1.404$ (400 °C); $R_B = 2.487$, $R_F = 1.508$ (500 °C). MEM nuclear density distribution maps on the (110) plane of $Bi_{12.5}Lu_{1.5}ReO_{24.5}$ at 25 °C and $Bi_{12.5}Er_{1.5}ReO_{24.5}$ at various temperatures are displayed in Fig. 4. Examination of nuclear density distribution suggests some cation disorder with slight displacements from their ideal *4a* position, but the most obvious feature concerns the disorder in oxide ions positions. As expected, the nuclear densities associated to oxide ions spread over a wide area, forming a continuous tetrahedral volume roughly covering the *8c* and *32f* positions, which is observed in other fluorite structured materials both experimentally [20,21] and theoretically [22]. This is observed at all studied temperatures and the extent of this volume increases with temperature, which is consistent with higher atomic displacement parameters at higher temperatures. Some differences can however be observed at different temperatures (Figs. 4 and 5).

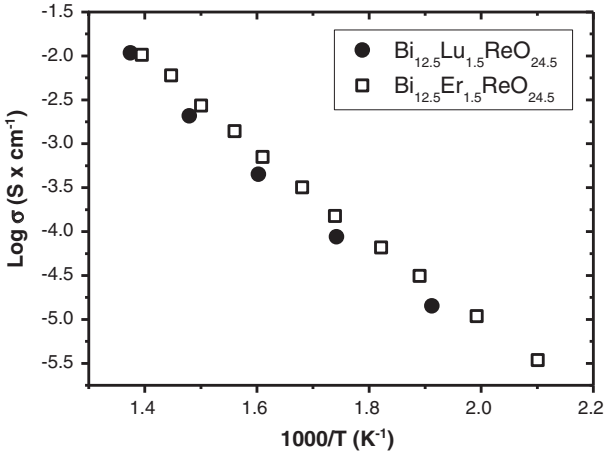

Fig. 1. Arrhenius plot of total conductivity for $Bi_{12.5}Lu_{1.5}ReO_{24.5}$ and $Bi_{12.5}Er_{1.5}ReO_{24.5}$.

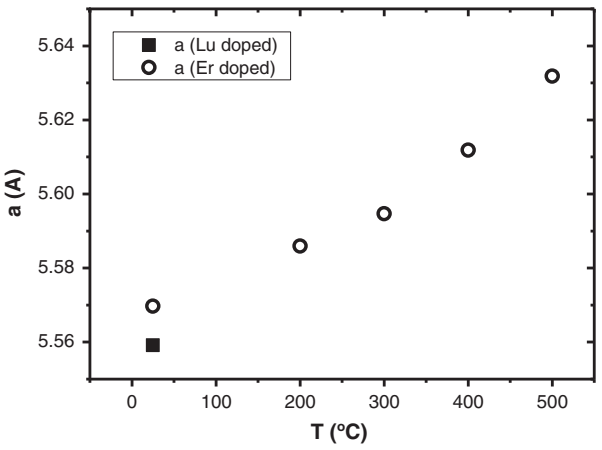

Fig. 2. Evolution of lattice parameter with temperature for $Bi_{12.5}Lu_{1.5}ReO_{24.5}$ and $Bi_{12.5}Er_{1.5}ReO_{24.5}$.

At 200 – 300 °C: nuclear densities are localised in the tetrahedral volume roughly covering the *8c* and *32f* positions with "bulges" of nuclear densities pointing toward the *48i* position, while at 400 and 500 °C continuous nuclear densities forming a straight line along the <100> direction are found, indicative of oxide-ion diffusion pathway along that direction. In the literature, curved pathways along the <100> direction passing through the *48i* site are generally observed in fluorite materials [20], the prevalence of curve pathway as opposed from straight pathway is explained by the repulsion between cation and anions, the curved pathway allowing the cation–anion to maintain a reasonable distance. However, a straight pathway is observed for $Y_{0.785}Ta_{0.215}O_{1.715}$ [23], as is the case for the present material. This suggests that Ta and Re cations might play a similar role in these systems.

The direct oxide-ion diffusion pathway along the <100> direction is visible at 400 and 500 °C, with coherent scattering length of 0.21 f. $Å^{-3}$ at the *24d* (0.5, 0.25, 0.25) site (distances cation – *24d* site ~1.99Å). Some density "bulges" from the tetrahedral volume covering the *8c* and *32f* sites pointing toward the <111> direction, and at the *24e* (0.33 0 0) site, are also present. This suggests a possible supplementary curved conduction path along the <110> direction going through the *8c/32f 24e 8c/32f* sites around the cation (distances cation – *24e* site ~1.86Å). Reducing the coherent scattering length to 0.11 f. $Å^{-3}$ allows visualising the pathway (Fig. 6).

It is interesting to note that the different nuclear densities associated to anion distribution at (i) 200–300 °C and (ii) 400–500 °C appear to reflect the non linear behaviour of atomic parameter variation with temperature. Non linear evolution of lattice parameter

Table 1
Final atomic positions for $Bi_{12.5}Lu_{1.5}ReO_{24.5}$ (BiLu) and $Bi_{12.5}Er_{1.5}ReO_{24.5}$ (BiEr) from Rietveld refinement. Space group *Fm-3m* (225); all cations in *4a* (*0 0 0*), O(1) in *8c* (¼ ¼ ¼), O(2) in *32f* (*x x x*). Cations occupancies Bi/Ln/Re = 0.8333/0.1/0.0667.

	BiLu- 25 °C	BiEr- 25 °C	BiEr- 200 °C	BiEr- 300 °C	BiEr- 400 °C	BiEr- 500 °C
a (Å)	5.5591(1)	5.5698(1)	5.5860(2)	5.5948(2)	5.6118(2)	5.6318(3)
x 32f	0.364(1)	0.368(1)	0.359(1)	0.356(1)	0.354(1)	0.354(1)
Occ O(1)	0.592(5)	0.586(5)	0.578(5)	0.568(5)	0.554(5)	0.554(6)
Occ O(2)	0.060(1)	0.053(1)	0.060(1)	0.062(1)	0.066(1)	0.066(1)
Uiso cations	4.55(4)	3.92(4)	5.33(3)	5.63(3)	6.21(4)	7.01(4)
Uiso oxygens	11.5(1)	10.2(1)	11.7(1)	11.8(1)	11.9(1)	12.6(1)
χ^2 *(47 var.)*	*2.409*	*2.780*	*3.478*	*3.304*	*2.887*	*2.696*
Rwp	*0.0246*	*0.0237*	*0.0274*	*0.0268*	*0.0251*	*0.0243*

with temperature in $Bi_3Ta_{0.50}Nb_{0.50}O_7$, resulting in slightly higher than expected cell volume at higher temperature, has been explained by the increased occupancy at the *24d* position – which is interstitial to the cubic closed packed (ccp) fluorite lattice – at elevated temperatures [19]. Since in the present materials nuclear densities are observed at the *24d* site at 400 and 500 °C only, this explanation can also be applied to the present case.

4. Conclusions

Both $Bi_{12.5}Lu_{1.5}ReO_{24.5}$ and $Bi_{12.5}Er_{1.5}ReO_{24.5}$ crystallise in the cubic δ-Bi_2O_3 type system. New information on the evolution with temperature in the oxygen sublattices of the highly disordered Bi–Ln–Re–O system has been collected. At 500 °C, an oxide ion diffusion pathway along <100> is clearly observed. Contrarily to most Bi_2O_3-

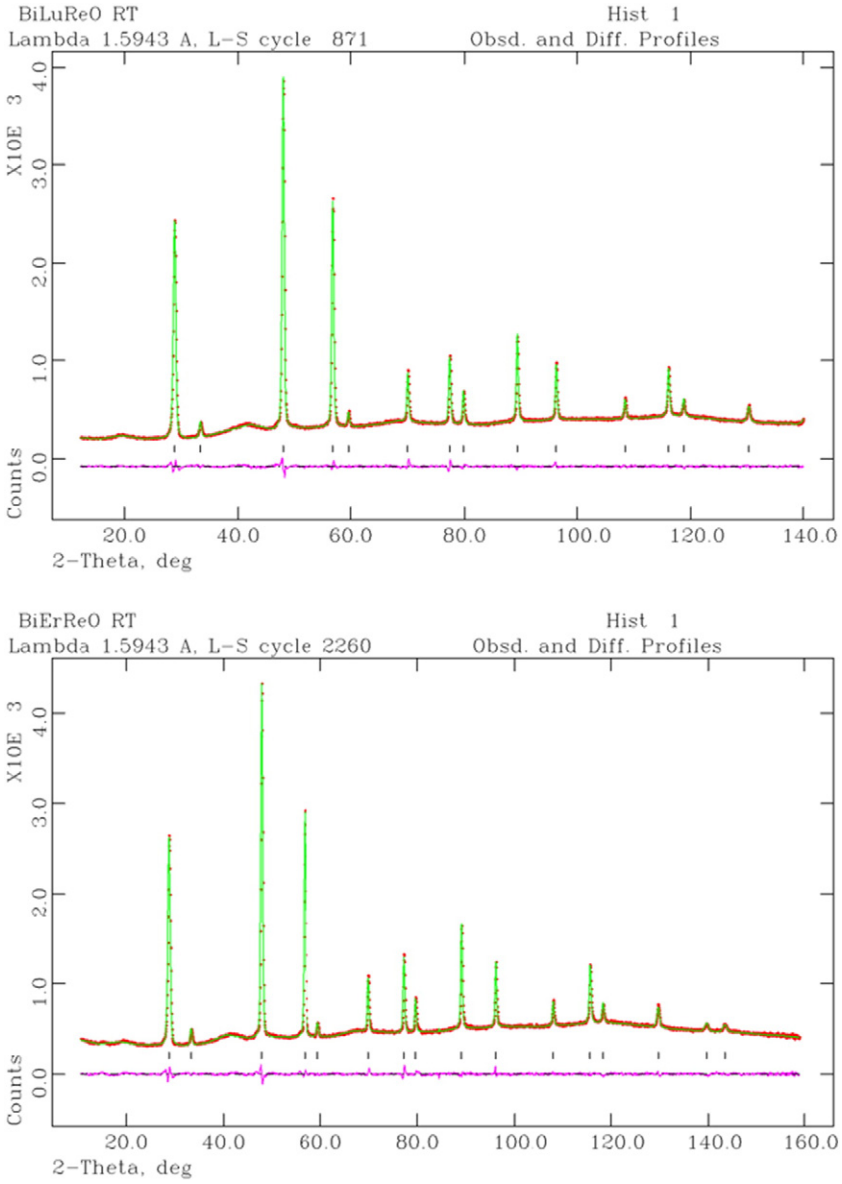

Fig. 3. Final Rietveld plot of a) $Bi_{12.5}Lu_{1.5}ReO_{24.5}$ and b) $Bi_{12.5}Er_{1.5}ReO_{24.5}$ at room temperature.

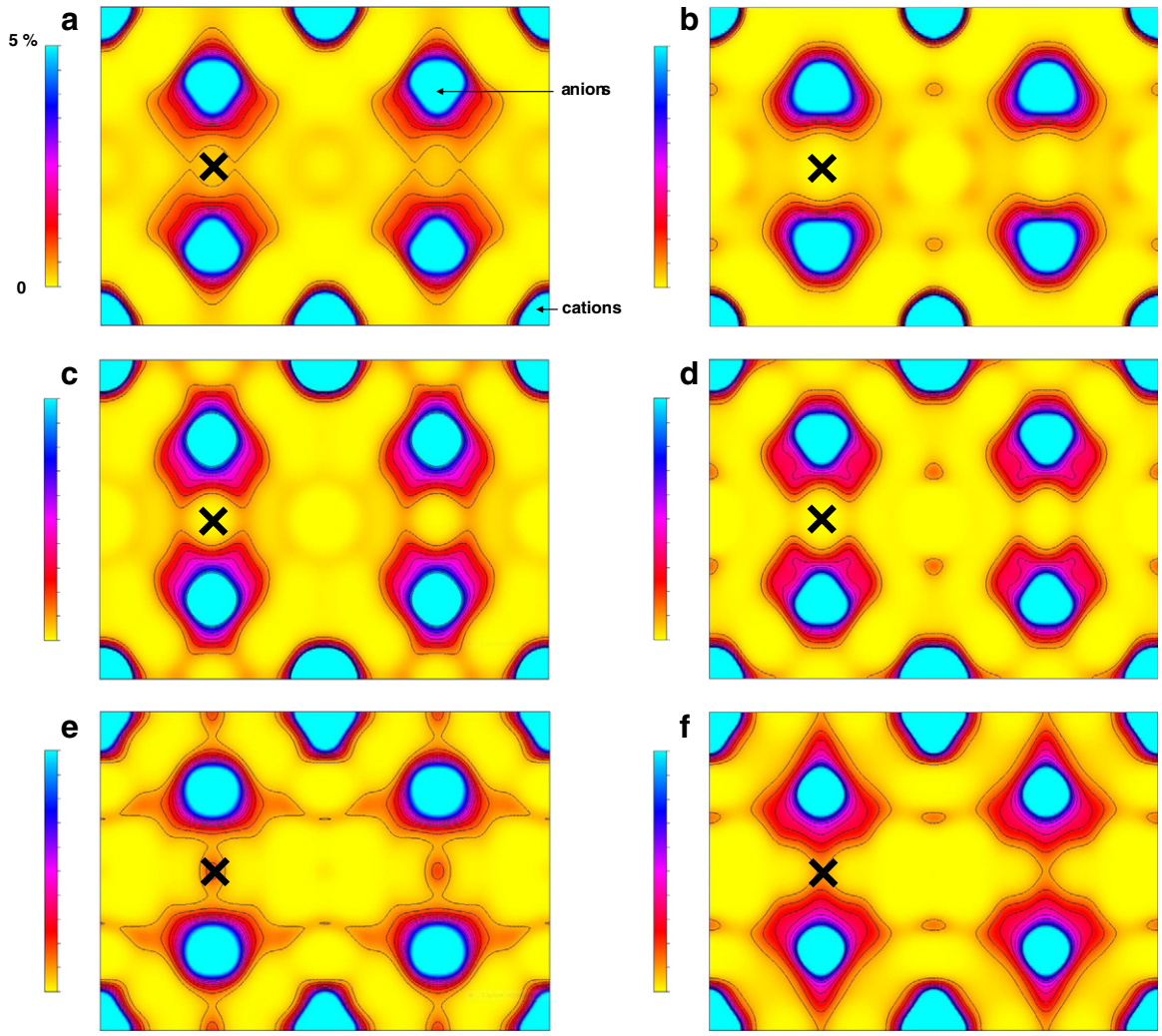

Fig. 4. Nuclear-density distribution on the (110) plane of a) $Bi_{12.5}Lu_{1.5}ReO_{24.5}$ at 25 °C and $Bi_{12.5}Er_{1.5}ReO_{24.5}$ at b) 25 °C, c) 200 °C, d) 300 °C, e) 400 °C, f) 500 °C. Saturation level 0 – 5%, with contours lines in the range 0.2 to 2 f. $Å^{-3}$ (0.2 f. $Å^{-3}$ step). The maximum densities corresponding to 100% are: for $Bi_{12.5}Lu_{1.5}ReO_{24.5}$: 53.91 f. $Å^{-3}$ at 25 °C; for $Bi_{12.5}Er_{1.5}ReO_{24.5}$: 51.04 f. $Å^{-3}$ at 25 °C, 38.31 f. $Å^{-3}$ at 200 °C, 44.52 f. $Å^{-3}$ at 300 °C, 53.20 f. $Å^{-3}$ at 400 °C, 43.32 f. $Å^{-3}$ at 500 °C. The black crosses indicate Wyckoff position 24d (0.5, 0.25, 0.25).

fluorite related systems, the pathway in the <100> direction is not curved but straight. An additional pathway in the <110> direction passing through the *24e* (~0.33 0 0) site is also suggested. These features would explain the enhanced oxide ion conductivity observed in these materials.

Acknowledgments

We thank EPSRC for financial support. We are grateful to Emmanuelle Suard at ILL for help with the collection of neutron diffraction data.

References

[1] G. Gattow, H. Schröder, Z. Anorg. Allg. Chem. 318 (1962) 176.
[2] P.D. Battle, C.R.A. Catlow, J. Drennan, A.D. Murray, J. Phys. C 16 (1983) L561.
[3] L.E. Depero, L. Sangaletti, J. Solid State Chem. 122 (1996) 439.
[4] M. Yashima, D. Ishimura, Chem. Phys. Lett. 378 (2003) 395.
[5] T. Takahashi, H. Iwahara, Mater. Res. Bull. 13 (1978) 1447.
[6] J.C. Boivin, G. Mairesse, Chem. Mater. 10 (1998) 2870.
[7] P. Shuk, H.-D. Wiemhöfer, U. Guth, W. Göpel, M. Greenblatt, Solid State Ionics 89 (1996) 179.
[8] R. Punn, A.M. Feteira, D.C. Sinclair, C. Greaves, J. Am. Chem. Soc. 128 (2006) 15386.
[9] R. Punn, I. Gameson, F. Berry, C. Greaves, J. Phys. Chem Solids 69 (2008) 2687.
[10] T.E. Crumpton, J.F.W. Mosselmans, C. Greaves, J. Mater. Chem. 15 (2005) 164.
[11] C.H. Hervoches, C. Greaves, J. Mater. Chem. 20 (2010) 6759.
[12] A.C. Larson, R.B. Von Dreele, General Structure Analysis System (GSAS), Los Alamos National Laboratory Report LAUR2004. 86–748.
[13] B.H. Toby, J. Appl. Crystallogr. 34 (2001) 210–213.
[14] F. Izumi, R.A. Dilanian, Recent Research Developments in Physics, Vol. 3, Part II, Transworld Research Network, Trivandrum, 2002, pp. 699–726.
[15] F. Izumi, K. Momma, Solid State Phenom. 130 (2007) 15–20.
[16] K. Momma, F. Izumi, J. Appl. Crystallogr. 44 (2011) 1272–1276.
[17] S. Boyapati, E.D. Wachsman, B.C. Chakoumakos, Solid State Ionics 138 (2001) 293.
[18] I. Abrahams, X. Liu, S. Hull, S.T. Norberg, F. Krok, A. Kozanecka-Szmigiel, M.S. Islam, S.J. Stokes, Chem. Mater. 22 (2010) 4435.
[19] M. Struzik, X. Liu, I. Abrahams, F. Krok, M. Malys, J.R. Dygas, Solid State Ionics 218 (2012) 25–30.
[20] M. Yashima, Solid State Ionics 179 (2008) 797–803.
[21] S. Hull, S.T. Norberg, M.G. Tucker, S.G. Eriksson, C.E. Mohn, S. Stølen, Dalton Trans. (2009) 8737–8745.
[22] C.E. Mohn, S. Stølen, S.T. Norberg, S. Hull, Phys. Rev. B 80 (2009) 024205.
[23] M. Yashima, T. Tsuji, Chem. Mater. 19 (2007) 3539–3544.

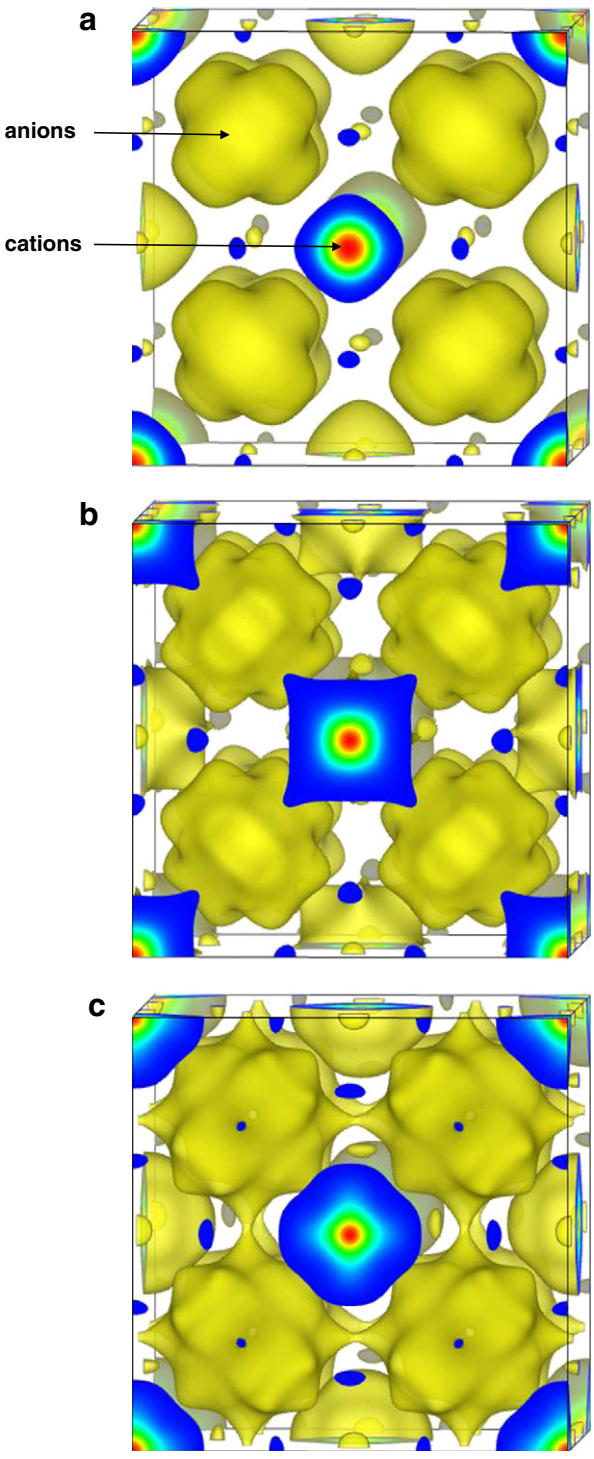

Fig. 5. 3D nuclear-density distribution of $Bi_{12.5}Er_{1.5}ReO_{24.5}$ at a) 25 °C, b) 300 °C, c) 500 °C. (0.2 f. $Å^{-3}$).

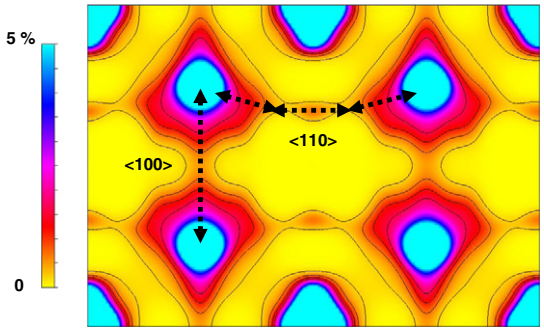

Fig. 6. Nuclear-density distribution on the (110) plane of $Bi_{12.5}Er_{1.5}ReO_{24.5}$ at 500 °C. Saturation level 0 – 5%, with contours lines in the range 0.1 to 2 f. $Å^{-3}$ (0.2 f. $Å^{-3}$ step). Arrows indicate apparent oxide ion diffusion paths along the 100 and 110 directions.